

Access graph: a novel graph representation of public transport networks for accessibility analysis

Tina Šfiligoj^{*1}, Aljoša Peperko², and Oded Cats³

¹Faculty of Maritime Studies and Transport, University of Ljubljana, Slovenia

²Faculty of Mechanical Engineering, University of Ljubljana and Institute of Mathematics, Physics and Mechanics, Slovenia

³Department of Transport & Planning, Delft University of Technology, The Netherlands

Abstract

Accessibility, defined as travel impedance between spatially dispersed opportunities for activity, is one of the main determinants of public transport (PT) use. In-depth understanding of its properties is crucial for optimal public transport systems planning and design. Although the concept has been around for decades and there is a large body of literature on accessibility operationalisation and measurement, a unified approach is lacking. To this end, we introduce a novel graph representation of public transport networks, termed the access graph, based on the shortest paths between nodes. Shortest paths are calculated using the in-vehicle time-weighted L- and frequency-weighted P-space representations to determine generalised travel times. Then there is an edge between two nodes in the access graph if the travel time between them is below a certain threshold time budget. In this representation, node degree directly measures the number of nodes reachable within a predetermined time. We study the threshold-dependent evolution of the access graph, focusing on average degree and degree distributions. Based on the topological properties of the access graph, we define a set of accessibility indicators. In addition, we propose indicators of access equity. We apply the methodology to a dataset of 51 metro networks worldwide. In all cases, a logistic-like growth of average degree with time budget is observed, indicating universal behaviour of accessibility and exhibiting the value of the proposed representation for unified accessibility studies and its potential for comparative analyses. We see a great potential for the access graph to drive in-depth studies of accessibility.

Keywords: public transport, accessibility, network science, metro network, equity

1 Introduction

Accessibility is key in providing individuals with the opportunity to take part in employment, education and recreational activities. The key objective of transport systems and public transport services in particular is therefore defined in terms of providing accessibility. The Hansen definition of accessibility as travel impedance between spatially dispersed opportunities for activity is at the core of defining accessibility indicators (Hansen, 1959; Geurs & Van Wee, 2004). It has been consistently in use since its conception as evident from a large body of literature, and has facilitated accessibility-based planning. Complementary to Hansen-like measures of access, also termed primal access, where travel time and number of reachable opportunities are the independent and dependent variable, respectively, dual access inverts the independent and dependent variables and measures the time needed to reach a predetermined number of nodes (Cui & Levinson, 2020).

Despite its wide theoretical and empirical developments, the exact role of accessibility remains somewhat unclear. While the general idea of accessibility is relatively straightforward, the concrete operationalisation and related indicators vary significantly across implementations. The exact definitions and functions of travel impedance differ, while determining reliable values for the number of opportunities is even more difficult to perform in a unified manner (Lahoorpoor et al., 2022).

This has led researchers to call for unified approaches to accessibility. Levinson & Wu (2020) proposed a general model across different modalities and categories of activity. This was followed by proposing a method which allows for the comparison of different modes of urban accessibility across different cities (Wu et al., 2021).

Graph-theoretical and network science approaches have been gaining in importance in public transport systems research. Although network science methods have been present in PTN research for almost four decades, having been introduced by Musso et al. (1988); Vuchic & Musso (1991), and

later advanced in a seminal paper by Von Ferber et al. (2009), there has been a widely recognised concern that this research has been driven primarily by network scientists using PTNs as real-world examples for theoretical developments (e.g. (Dupuy, 2013)). As a result, the practical implications for transportation researchers and planners have often been overlooked.

Recently, this gap has begun closing down with transport researchers increasingly using network science approaches in modelling and studying PTN properties (Derrible & Kennedy, 2011; Ding et al., 2019). This is especially evident in network robustness and vulnerability studies (Adjetei-Bahun et al., 2016; Cats, 2016; Cats et al., 2017; Cats & Krishnakumari, 2020). In contrast, network-based accessibility research has received comparatively less attention. Past studies focused either on analyzing the relative importance of nodes using centrality indicators (Cats, 2017; Šfiligoj et al., 2025) or compared different networks using an aggregate metric such as the average shortest path from each node to all other nodes, known as network (in)efficiency (Dimitrov & Ceder, 2016; de Regt et al., 2019). In a pioneering study, Luo et al. (2019) suggested connecting network science and accessibility by calculating average shortest paths for each node to all other nodes, providing a Hansen-like indicator similar to closeness centrality. Their application of the method to eight tram networks worldwide demonstrated the potential of network-based methods for comparative assessment. As evident from recent literature, the increasing availability of standardised timetable data in the General Transit Feed Specification (GTFS) format has made accessibility studies increasingly accessible (GoogleDevelopers, 2025).

In the present work, we advance the argument for using graph-theoretical approaches for accessibility research. Accessibility is fundamentally about connectedness, which is naturally modelled with graphs. We argue that previous approaches that used aggregated values such as node centrality do not provide a sufficiently complete and insightful information when comparing accessibility across networks. First, centrality measures, even those in which the global properties of the network are implicit in their definition, offer a local and isolated node-level metrics. Second, centrality measures originate from social network analysis, and while they have been used successfully in PT studies, their interpretation in the transport context may be obscured to some extent. This may consequently limit the generalisation of these measures to potential new models, such as including land use, and thereby diminish their interpretability.

To address the above-mentioned shortcomings, we propose a novel graph representation, called the access graph, where two nodes share an edge if they can be reached from one another within a given travel time budget. The matrix of generalised travel times is based on two standard PTN representations, the so-called L- and P-space representations, where nodes represent service stops. In L-space, or space-of-infrastructure, there is an edge between two nodes if they represent consecutive stops on a line, whereas in P-space, or space-of-service, there is an edge between each pair of nodes lying along the same line, reflecting the ability of passengers to travel between nodes without transfer. Edge weights may represent in-vehicle and waiting time, for L-space and P-space, respectively (Luo et al., 2020). The distance matrices of the corresponding representations are used to calculate generalised travel times.

Importantly, in the resulting graph representation, while retaining the same set of nodes, the edges directly indicate accessibility between two nodes. Specifically, node degree in the access graph directly provides the number of reachable nodes within a specific time budget limit. Based on this representation, we study the temporal dependence of node degree distributions, focusing on average degree. Furthermore, access equity is among the most pressing issues in accessibility-based design, where large (spatial) disparities in access to PT impact available opportunities for different social groups (Neutens, 2015; El-Geneidy et al., 2016; Karner, 2018; Bittencourt & Giannotti, 2023). To this end, the Gini coefficient of the degree distribution is used as an indicator of access inequality (Gori et al., 2020).

The contribution of this study is threefold:

1. **Methodological:** We introduce a novel PTN graph representation, the *access graph*, which connects pairs of nodes based on their reachability on generalised time-weighted shortest paths. This is the principal contribution of this work.
2. **Applied:** Based on the topology of the access graph, we define a set of accessibility indicators, including access inequality indicators.
3. **Empirical:** We apply the methodology to a dataset of 51 metro networks worldwide to study the properties of the access graph and compare accessibility measures across networks.

The remainder of this study is structured as follows. In Section 2, the methodology of construction of the access graph and definitions of the proposed indicators is detailed. In Section 3,

the results of the empirical analysis on the metro dataset are presented. Section 4 concludes this study and offers directions for further research.

2 Methodology

2.1 Preliminaries

A graph is a structure $G(V, E)$ with a set of vertices, or nodes, $V = \{v_1, \dots, v_N\}$ and a set of edges $E = \{e_{ij}\}$, where an edge $e_{ij} = (v_i, v_j)$ connects nodes v_i and v_j . $N = |V|$ and $M = |E|$ are the dimension and the size of the graph, respectively. A graph with no edges is an empty graph, and a graph where all pairs of nodes share an edge, is a complete graph, or a clique. A graph is most commonly represented in matrix form with the adjacency matrix A of dimension $N \times N$ and with entries $a_{ij} = 1$ if there is an edge between nodes i and j , and $a_{ij} = 0$ otherwise. A weighted representation provides a generalisation where edges are assigned weights, corresponding to their properties (e.g. cost or strength of connection). Node degree $D(i)$ of node i counts the number of the node's direct neighbours, and equals the sum of the corresponding row in the adjacency matrix, $D(i) = \sum_{j=1}^N a_{ij}$. If the graph is connected, the $N \times N$ matrix \mathcal{D} of the graph contains as elements d_{ij} the lengths of the shortest paths between all pairs of nodes.

Many real-world systems, among them (public) transport systems, can be modelled as networks, comprising of sets of elements and their interconnections. A network is modelled as a graph that possesses certain properties of the real-world objects represented by nodes and edges.

2.2 Access graph

In PT access studies, generalised travel time is typically comprised of in-vehicle and waiting times, together with transfer costs. In the access graph \mathcal{G}_A , the nodes represent the stops of a PTN, and the edge set is obtained depending on the generalised travel times as follows. First, the generalised travel time matrix \mathcal{D} is constructed:

1. Construct the standard graph representations: frequency-weighted P-space representation with edge weights representing service frequencies f_{ij} (given as number of rides per hour) and in-vehicle time-weighted L-space representation with edge weights t_{ij}^L .
2. Transform the edge weights of the P-space representation into average waiting time t^{wait} in minutes, defined as half of the headway: $t_{ij}^{wait} = 30/f_{ij}$.
3. Assign in-vehicle time weights t_{ij}^{in-veh} to P-space edges by calculating the weight of the corresponding path in L-space (summing in-vehicle times on all consecutive links).
4. Calculate the distance matrix $\mathcal{D}^{P^{wait}}$ of the waiting time-weighted P-space representation.
5. Determine the distance matrix of in-vehicle times $\mathcal{D}^{P^{in-veh}}$ by calculating the in-vehicle time weights of the paths obtained in the previous step.
6. Similarly, determine the distance matrix \mathcal{D}^{P^u} of corresponding path lengths in unweighted P-space. Note that $([\mathcal{D}^{P^u}]_{ij} - 1)$ counts the number of transfers along the path between i and j .
7. Construct the generalised travel time matrix \mathcal{D} :

$$\mathcal{D} = \mathcal{D}_{L^{in-veh}} + w^{wait} \mathcal{D}_{P^{wait}} + w^{transfer} (\mathcal{D}_{P^u} - J_N), \quad (1)$$

where J_N is an $N \times N$ matrix of ones, $w^{wait} = 2$ is the waiting time weight and $w^{transfer} = 5$ min is the transfer penalty. The values are determined from the literature and reflect average passengers' valuation of time (Yap et al., 2024).

Note that the entry $d_{ij} = [\mathcal{D}]_{ij}$ of the generalised travel time matrix represents the generalised travel time between stops i and j . In the next step, the time budget t_b is introduced, i.e. the maximum total travel time allowed. Then there exists an edge between nodes i and j if and only if $d_{ij} \leq t_b$. The adjacency matrix A with entries a_{ij} of the access graph is thus obtained from the generalised travel time matrix:

$$a_{ij} = \begin{cases} 1 & d_{ij} \leq t_b \\ 0 & \text{otherwise} \end{cases} \quad (2)$$

The edge set of the access graph is thus time-budget dependent. \mathcal{G}_A obtained in this process is an undirected unweighted graph. Although the standard graph representations are implicit in its construction, the edges connect nodes reachable within the time budget by following the shortest path. Therefore, node degree D of \mathcal{G}_A is a direct measure of stop-level accessibility. Specifically, it provides a gravity-type measure, using a time-based cut-off function.

2.3 Access indicators

The evolution of the access graph is observed with increasing the time budget t_b from 0 to $t_{max} = \max_{i,j} d_{ij}$. At $t_b = 0$ \mathcal{G}_A is an empty graph, and at $t_b = t_{max}$, \mathcal{G}_A is a complete graph. The average degree \bar{D} in these boundary cases is 0 and $N - 1$, respectively. To examine global accessibility indicators, the shape of the average degree growth with increasing t_b in the interval $[0, t_{max}]$ is studied.

For almost all cities in our empirical analysis, a logistic-like convergence to the maximum degree is observed. Thus, there is a point where the rate of average degree growth starts to decrease. In a continuous limit, this would correspond to the point of inflection, where a function changes from convex to concave, or vice-versa, and where typically the second derivative is zero. Importantly (in the logistic-shape example), this corresponds to the point at which the first derivative reaches a maximum. While the access graph describes cumulative accessibility, the first derivative approximation gives an indication of interval accessibility (i.e. number of nodes reachable in the time interval $[t_b(k), t_b(k + 1)]$, where k is the time step counter). Here, we are working with numerical approximations and use difference quotients $\frac{\Delta \bar{D}}{\Delta t_b}$ as approximations of the derivatives. In data, non-smooth first-order difference quotients, together with multiple points of inflection are observed for several networks included in our analysis. Thus, to devise a robust indicator, the time budget at the global maximum of $\frac{\Delta \bar{D}}{\Delta t_b}$ is used. Note that this corresponds to the time interval with the highest interval accessibility.

From the access perspective, the point where the maximum of the first derivative is achieved, is interesting. This point can be understood as the time where the network has reached an "accessible state" after which the connections between the remaining pairs of nodes emerge at a (distinctively) lower rate. Based on this reasoning, three global accessibility indicators are proposed. First, the time budget at the occurrence of the point of maximum growth, t_M , is proposed as an absolute-value indicator. The reasoning behind this choice is that the individual time budget does not increase, or increases only marginally, with city size (Ahmed & Stopher, 2014). To incorporate the effects of network size, an additional indicator δt_M is proposed that measures the point of maximum growth relative to the maximum generalised travel time observed in the network, i.e. $\delta t_M = t_M / t_{max}$. Since both t_M and t_{max} vary across networks, using both t_M and δt_M as separate indicators offers a way to disentangle the effects of both variables. Moreover, the former emphasises the (approximately) universal passenger travel time budget, and the latter reflects network performance properties. Note that lower values of t_M and δt_M generally imply higher accessibility.

In addition to the values of the (relative) time budgets at maximal growth, the value of the average degree at t_M , \bar{D}_M , constitutes an additional indicator. This represents a set of complementary indicators, with t_M and δt_M measuring dual access, and \bar{D}_M a corresponding primal access indicator.

In addition, we investigate the average degree of the access graph when the time budget is equal to 30 minutes, \bar{D}_{30} . Our interest in this specific travel time budget stems from the proposition that in urban areas, most of trips are assumed to be parts of a home-activity tour, and the maximum daily individual time budget is approximately one hour (Ahmed & Stopher, 2014).

Alongside the average degree, we examine the t_b -dependent degree distributions of the access graph for the purpose of access equity assessment. A standard measure of inequality is the Gini coefficient, defined as:

$$G = \frac{\sum_{i=1}^n \sum_{j=1}^n |x_i - x_j|}{2n^2 \bar{x}}, \quad (3)$$

where $\bar{x} = \frac{1}{n} \sum_{i=1}^n x_i$ is the distribution mean (Gori et al., 2020). G can assume values in the interval $[0, 1]$, where $G = 0$ represents perfect equity and $G = 1$ means maximum disparity. In this study, the values of the Gini coefficients of the node degree distributions of the access graph are observed. Following a similar reasoning as above, G_M and G_{30} , representing the values of the Gini coefficients of the degree distribution of the access graph at $t_b = t_M$ and $t_b = 30$ min, respectively, are proposed as indicators of access inequality. The Gini coefficient is chosen here rather than

skewness, because the degree distributions in our empirical analysis were found to often exhibit a bimodal shape. The accessibility indicators used in the analysis are summarised in Table 1.

Table 1: Accessibility indicators used in the analysis.

Notation	Definition
t_M	time budget at maximum growth of average degree
δt_M	t_M/t_{max} ; t_M relative to maximum generalised travel time
\bar{D}_M	average degree of the access graph at t_M
\bar{D}_{30}	average degree of the access graph at $t_b = 30$ min
G_M	the Gini coefficient of the degree distribution at t_M
G_{30}	the Gini coefficient of the degree distribution at $t_b = 30$ min

3 Results and analysis

The proposed methodology is applied to a dataset of metro networks of 51 cities worldwide. We use publicly available in-vehicle time-weighted L-space and frequency-weighted P-space representations which were constructed using GTFS data (Vijlbrief et al., 2022a,b). For each metro network, access graphs are built for varying time budgets. t_b is varied in the interval $[0, t_{max}]$, where t_{max} is the maximum generalised travel time in the network, with progressively increasing steps of 2 minutes. The Python NetworkX library was used for graph construction and analysis (Hagberg et al., 2008). In the following, we first in Section 3.1 provide a detailed explanation of the results for the example of the Amsterdam metro. Section 3.2 then presents the results of the empirical analysis for the full metro dataset.

3.1 Illustration: the case of the Amsterdam metro

The Amsterdam metro network has $N = 39$ nodes, and a maximum generalised travel time of $t_{max} = 54$ minutes. The dependence of degree distributions and average degree on the time budget is represented with a heatmap (see upper plot in Figure (1)). The x -axis represents the time budget t_b , and y -axis represents the degree D in the respective access graph. The width of t_b and D bins is 2 minutes and 2, respectively. The colors of the heatmap cells represent the percentage of nodes in each degree bin. For clarity, the degree distributions at three selected values of the time budget, $t_b = \{6, 12, 18\}$ minutes, are also shown in the form of histograms in the respective subplots in the bottom row of Figure (1). At lower values of t_b , the degree distribution will be skewed to the left, which is demonstrated at $t_b = 12$ min with a peak of 17 nodes in the $D = 6$ bin, also seen as a dark blue cell in the heatmap. There is still a number of nodes with degree 0 or 1 (7 nodes) and only 2 nodes with degree in $D \in [8, 9]$. As the travel time budget increases, the values of the average degree, along with the minimum and maximum degree, increase and the degree distribution is progressively skewed to the right. At $t_b = 36$ min, there is a peak at the maximum node degree, and there are no nodes with degree below 15. The distribution reaches the widest span between minimum and maximum values at intermediate time steps, as seen for $t_b = 24$ min among the chosen values.

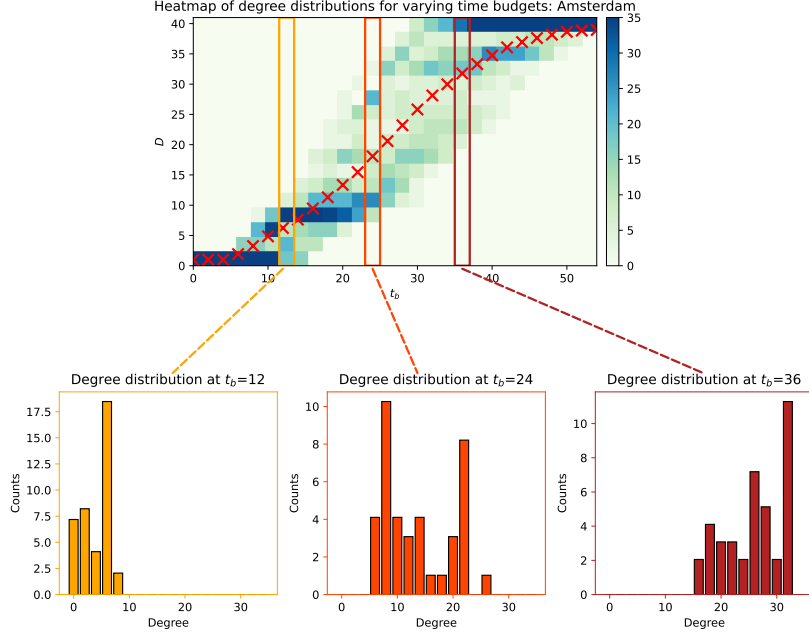


Figure 1: Results for the example of the Amsterdam metro network. The upper plot shows the heatmap of degree distributions with varying time budgets. t_b is increased in steps of 2 minutes. The x -axis represents the time budget, and the y -axis represents the node degree in the respective access graph. Heatmap cell color represents the percentage of nodes in each degree bin. Thus, each vertical column represents the color-coded histogram of the node degree distribution. The average degree at each t_b bin is plotted with red markers. For three selected values of the time budget, $t_b = \{6, 12, 18\}$, the heatmap visualisation is translated into the node degree histograms in the three bottom plots.

A visualisation of the evolution of the access graph with t_b for the Amsterdam metro is shown in Figure (2). The top left plot shows the L-space representation of the Amsterdam metro. In subsequent plots, the access graphs at 14 selected values of t_b are shown. In the first two plots, G_A is an empty graph, meaning that at $t_b = 4$ min no pairs of nodes exist, i.e. there is no pair of stations which are reachable within that generalised travel time budget. Consequently, the average degree $\overline{D} = 0$ in the first three columns of the heatmap. At $t_b = 8$ min edges begin to appear, connecting the fastest reachable pairs of nodes. For the Amsterdam metro, $t_M = 29$ min, i.e. up to which point there is an increasing growth of average degree. After that point, the growth begins to slow down. At $t_b = t_{max} = 54$ min, G_A is a complete graph with $\overline{D} = 38$, as also seen in the last t_b bin of the heatmap in Figure (1)).

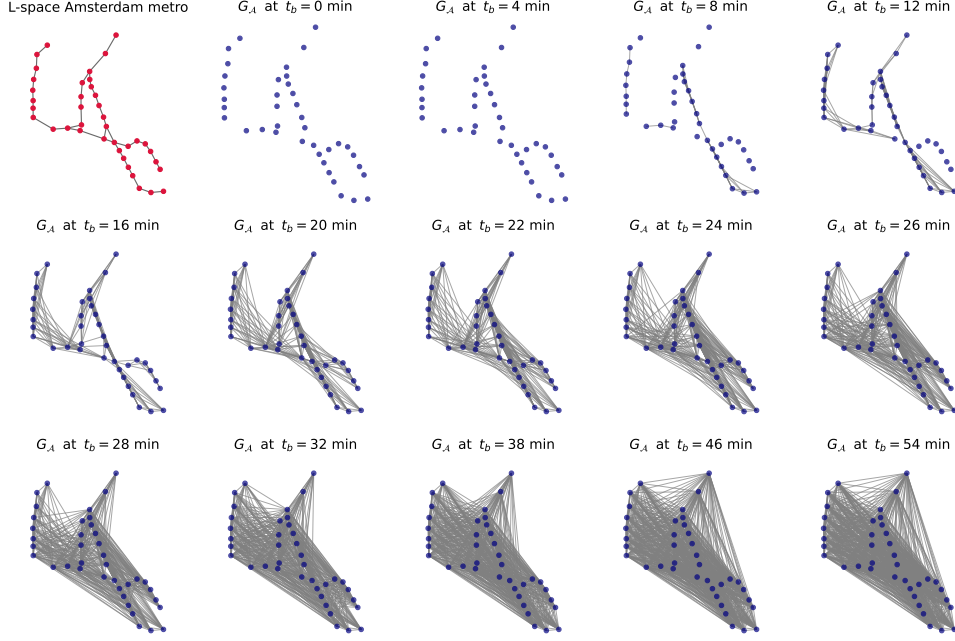


Figure 2: A visualization of the time budget-dependent access graph for the Amsterdam metro. In the top left plot is the L-space representation. In subsequent plots, access graphs at respective values of t_b , as indicated in each subplot title, are shown. The Amsterdam metro has $N = 39$ nodes and a maximum generalised travel time of $t_{max} = 54$ min.

3.2 Results for the metro dataset

This section presents the results for all 51 metro networks included in our analysis. The results of the average degree and degree distribution analysis as described in the previous section (3.1) are shown for all metros in Figure 3. Each of the subplots represents a separate network (city) and shows the time evolution of the access graph with the heatmaps representing node degree distributions. Average degree at each t_b bin is plotted with red markers.

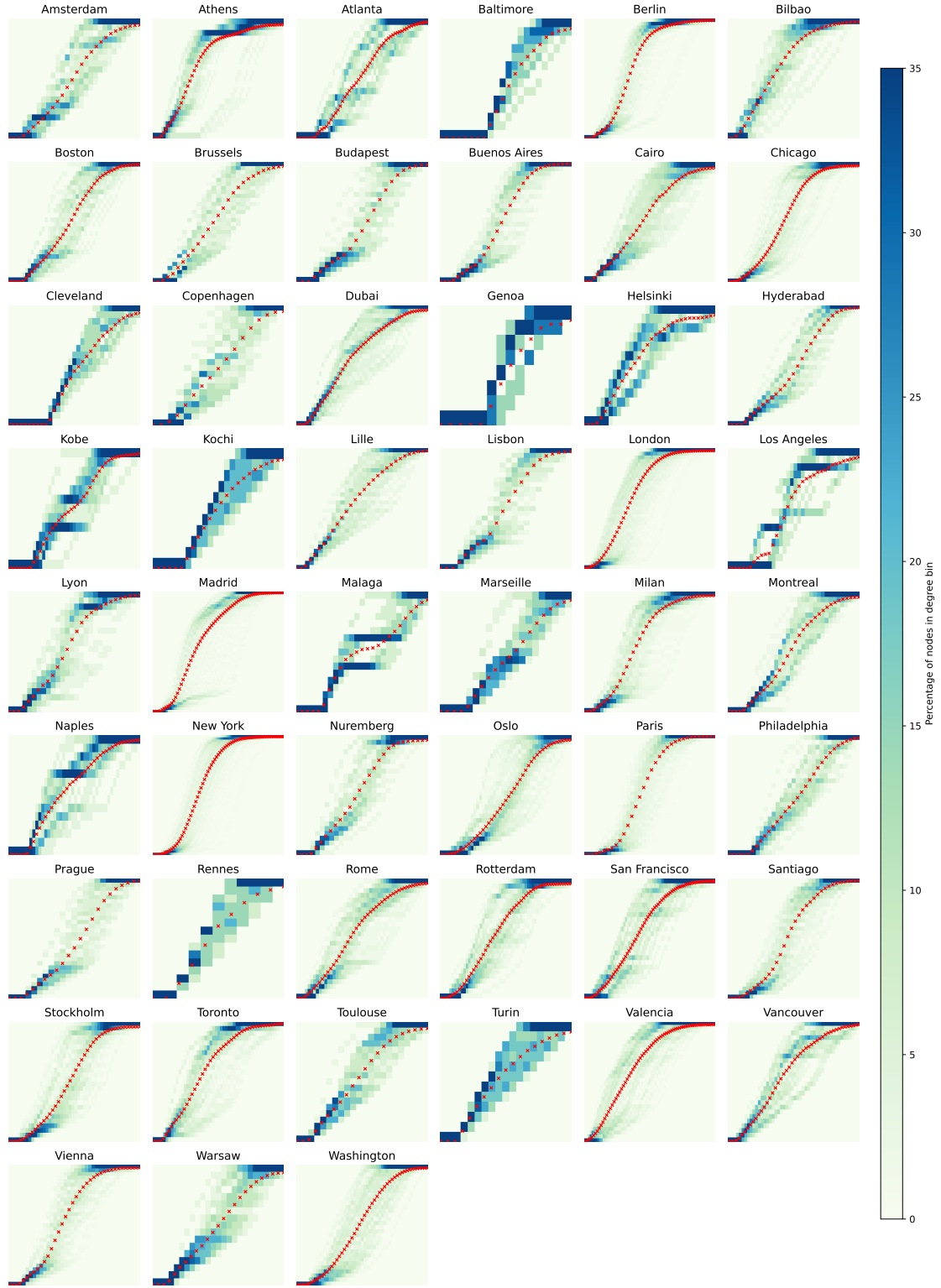


Figure 3: Degree distributions of access graphs with varying t_b . Each subplot shows the time evolution of the access graph with the heatmaps representing node degree distributions. t_b is increased in steps of 2 minutes. In each subplot, the x -axis represents the time budget, and y -axis represents the degree in the corresponding access graph. Heatmap cell colors represent the percentage of nodes in each degree bin. Average degree of the access graph at t_b is shown with red markers.

In almost all cases, a logistic-like S -shaped convergence of average degree \bar{D} to the maximum degree is observed. The most regular S -shaped behaviour is observed for the largest networks (New York, London and Paris, among others). In these cases, the value of t_M corresponds to the

inflection point (i.e. the "turning point" of the S -curve). Several networks exhibit a more complex behaviour with multiple points of inflection in $\overline{D}(t_b)$ (e.g. Athens, Los Angeles and Naples), implying several local extrema of $\overline{D}(t_b)$. The detailed exploration of the growth of the average degree is outside the scope of this study, however, we suggest line-level effects (e.g. line length and the importance of transfers in connecting node pairs) and the general topology of the L-space graph as likely predictors of this behaviour.

To define a robust measure, the t_b at the global maximum of the first difference quotient was chosen as the value of the t_M indicator. Figure (4) shows the rate of growth of the average node degree $y = \frac{\Delta \overline{D}}{\Delta t_b}$, calculated in discrete steps of 2 minutes. For example, for the New York metro, the maximum change of $y \approx 8$ is observed at $t_b = 51$ min. This means that when the time budget is increased from 50 to 52 minutes, the average degree of the access graph increases by approximately 16, or 8 per minute, on average. The middle of the interval where this is achieved is taken as the accessibility indicator t_M , meaning $t_M = 51$ min for the New York metro network.

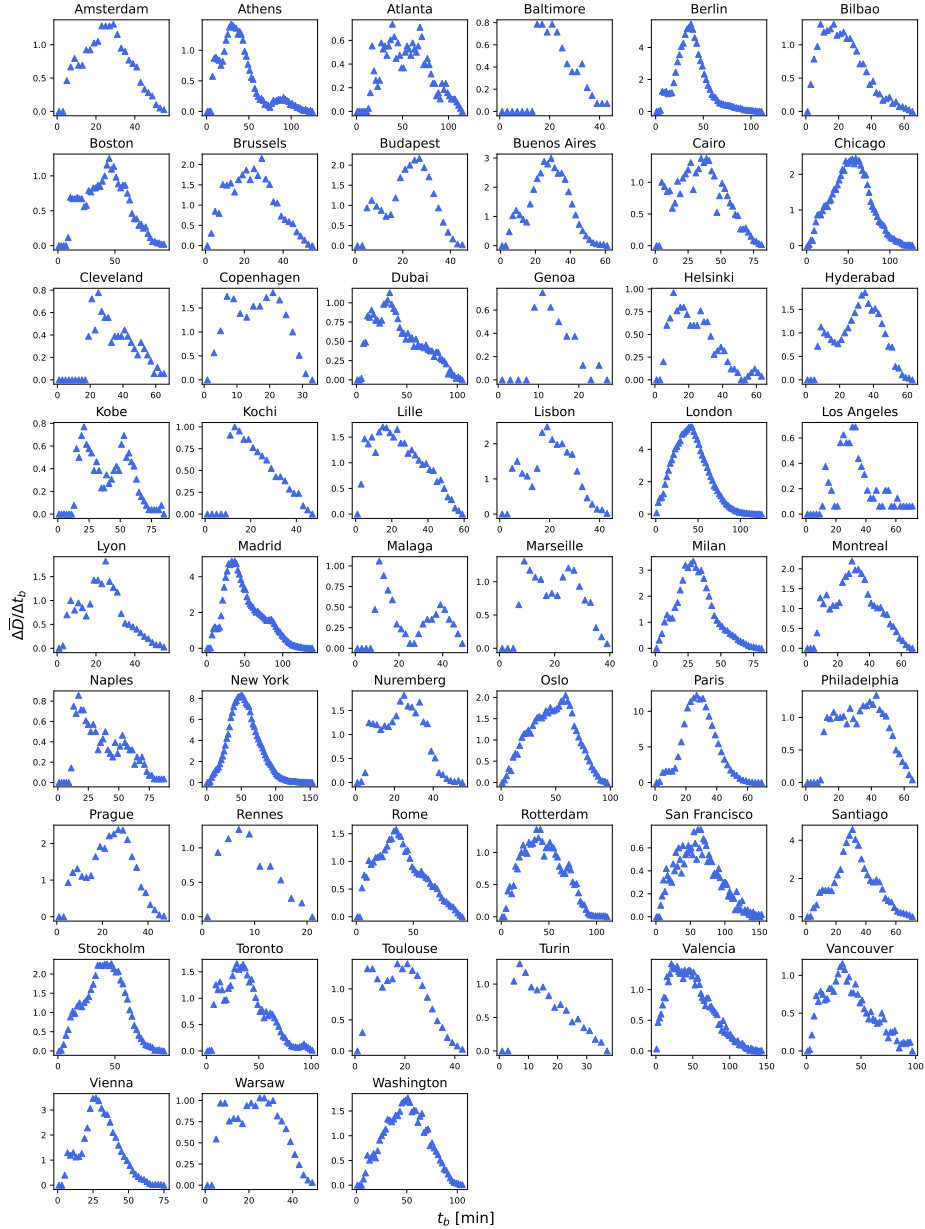


Figure 4: Rate of growth - the first difference quotient - of the average node degree $\frac{\Delta \overline{D}}{\Delta t_b}$ on the y -axis vs. generalised travel time budget t_b on the x -axes, calculated in discrete steps of 2 minutes. The value of t_b where y reaches the global maximum is taken as the value of t_M .

The numerical values of all indicators are summarised in Table 2. The networks are of remarkably diverse dimensions, ranging from $N = 8$ (Genoa) to $N = 421$ (New York). Maximum generalised travel time ranges from $t_{max} = 20$ (Rennes) to $t_{max} = 152$ minutes (New York, San Francisco). Large metropolitan areas are expected to have large values of t_{max} , e.g. 120 and 138 minutes for London ($N = 261$) and Madrid ($N = 240$), respectively. An exception is Paris with $N = 303$ and $t_{max} = 66$ min, suggesting a high level of accessibility. On the other hand, moderately sized networks with high values of t_{max} , e.g. Valencia ($N = 95, t_{max} = 140$), Chicago ($N = 137, t_{max} = 126$) or Athens ($N = 61, t_{max} = 120$) are less accessible, with the extreme case of San Francisco with $N = 50$ and $t_{max} = 152$.

Nine of the networks comprise of a single line: these are the metros in Baltimore, Cleveland, Genoa, Helsinki, Kochi, Los Angeles, Malaga, Rennes, and Turin. Their dimension ranges from 8 (Genoa) to 25 (Helsinki). For one-line networks, the growth of the access graph depends only on in-vehicle times as there are no transfers and waiting time is constant for the whole network.

The time at the largest degree growth ranges from $t_M = 7$ (Rennes) to $t_M = 61$ minutes (San Francisco). Note that almost half of the networks (23 networks) have t_M in the interval between 25 and 35 minutes, meaning that the operational characteristic time is close to the passengers'-oriented value of 30 minutes. The values of δt_M range from 0.15 (Valencia) 0.66 (Copenhagen). Note that low values of δt_M do not directly imply high accessibility, as is seen in the case of Valencia with the value of $\bar{D}_M = 0.19$. Conversely, the Copenhagen metro reaches the highest value among networks with $\bar{D}_M = 0.75$ and is one of the best connected networks with $t_{max} = 32$ and $t_M = 21$ minutes at $N = 39$. The lowest average degree at t_M is $\bar{D}_M = 0.14$ for Marseille, and the largest $\bar{D}_M = 0.75$ for Copenhagen ($\bar{D}_M = 0.73$ for Oslo). In comparison, the average degree at $t_b = 30$ min ranges from $\bar{D}_{30} = 0.11$ for New York to $\bar{D}_{30} = 0.97$ for Copenhagen.

Next, we turn to investigating access equity. Values of G_M and G_{30} are in the interval between ≈ 0.05 and ≈ 0.4 , with the exception of networks with $t_{max} \lesssim 30$ min where $G_{30} = 0$. This happens for two of the one-line networks, Rennes and Genoa, as well as Copenhagen. The value of $G_M = 0.14$ is a further indicator of the quality of the Copenhagen metro. The highest disparities are observed for Valencia ($G_M = 0.40, G_{30} = 0.33$) and Madrid ($G_M = 0.37, G_{30} = 0.40$). The largest value of $G_{30} = 0.42$ is observed for New York, however, with its large size and maximum travel time, this is expected and the value $G_M = 0.25$ indicates moderate inequality.

For the illustrative example of the Amsterdam metro in the previous section (3.1), the values of the accessibility indicators are: $t_M = 29$ min, $\delta t_M = 0.54$, $\bar{D}_M = 0.64$, $\bar{D}_{30} = 0.64$, $G_M = 0.20$, $G_{30} = 0.20$, indicating high global levels of accessibility and a high degree of equity in access distribution across the network. Among networks of similar dimension, the overall accessibility levels of the Amsterdam network are somewhat below those of the Copenhagen and Toulouse networks, comparable to the Lyon metro, and significantly outperforming the Atlanta network.

Table 2: Values of the studied variables for each network (city). N : number of nodes in the network; t_{max} : maximum generalised travel time (in minutes); t_M : time of maximum average degree growth (in minutes); $\delta t = \frac{t_M}{t_{max}}$; \bar{D}_M : average degree at t_M ; \bar{D}_{30} : average degree at $t_b = 30$ min; G_M : Gini coefficient at t_M ; G_{30} : Gini coefficient at $t_b = 30$ min.

City	N	t_{max}	t_M	δt_M	\bar{D}_M	\bar{D}_{30}	G_M	G_{30}
Amsterdam	39	54	29	0.54	0.64	0.64	0.18	0.18
Athens	61	120	31	0.26	0.45	0.40	0.27	0.28
Atlanta	38	114	39	0.34	0.31	0.16	0.27	0.38
Baltimore	14	42	21	0.50	0.44	0.73	0.16	0.11
Berlin	174	108	37	0.34	0.55	0.31	0.22	0.29
Bilbao	42	64	17	0.27	0.40	0.72	0.20	0.13
Boston	52	92	45	0.49	0.56	0.26	0.21	0.25
Brussels	59	52	29	0.56	0.70	0.70	0.16	0.16
Budapest	48	44	25	0.57	0.60	0.77	0.20	0.13
Buenos Aires	78	60	29	0.48	0.57	0.57	0.21	0.21
Cairo	61	80	35	0.44	0.53	0.40	0.22	0.24
Chicago	137	126	49	0.39	0.45	0.16	0.29	0.37
Cleveland	18	64	25	0.39	0.26	0.39	0.11	0.10
Copenhagen	39	32	21	0.66	0.75	0.97	0.14	0.00
Dubai	53	102	33	0.32	0.44	0.36	0.17	0.19
Genoa	8	26	11	0.42	0.34	0.88	0.28	0.00
Helsinki	25	62	11	0.18	0.20	0.70	0.28	0.14
Hyderabad	56	60	35	0.58	0.62	0.43	0.17	0.19
Kobe	26	84	21	0.25	0.20	0.37	0.26	0.19
Kochi	21	46	13	0.28	0.18	0.75	0.12	0.11
Lille	60	58	15	0.26	0.32	0.66	0.17	0.15
Lisbon	50	42	19	0.45	0.48	0.86	0.22	0.08
London	261	120	41	0.34	0.56	0.31	0.24	0.37
Los Angeles	16	70	31	0.44	0.52	0.42	0.16	0.20
Lyon	40	54	25	0.46	0.60	0.74	0.20	0.14
Madrid	240	138	33	0.24	0.31	0.23	0.37	0.40
Malaga	17	48	11	0.23	0.18	0.55	0.13	0.14
Marseille	29	38	9	0.24	0.14	0.83	0.17	0.08
Milan	106	80	29	0.36	0.51	0.51	0.26	0.26
Montreal	67	66	33	0.50	0.60	0.48	0.17	0.21
Naples	28	86	17	0.20	0.17	0.44	0.34	0.23
New York	421	152	51	0.34	0.49	0.11	0.25	0.42
Nuremberg	49	54	25	0.46	0.55	0.68	0.20	0.17
Oslo	101	92	59	0.64	0.73	0.22	0.15	0.30
Paris	303	66	27	0.41	0.49	0.57	0.25	0.22
Philadelphia	50	64	39	0.61	0.63	0.40	0.14	0.18
Prague	58	44	27	0.61	0.66	0.75	0.18	0.14
Rennes	15	20	7	0.35	0.44	0.93	0.12	0.00
Rome	73	92	35	0.38	0.48	0.36	0.21	0.24
Rotterdam	70	110	39	0.35	0.45	0.27	0.24	0.28
San Francisco	50	152	61	0.40	0.53	0.16	0.23	0.35
Santiago	119	70	31	0.44	0.52	0.44	0.22	0.25
Stockholm	101	90	45	0.50	0.62	0.27	0.21	0.33
Toronto	75	100	29	0.29	0.40	0.40	0.28	0.28
Toulouse	37	42	21	0.50	0.63	0.86	0.16	0.07
Turin	23	36	7	0.19	0.20	0.90	0.09	0.04
Valencia	95	140	21	0.15	0.19	0.31	0.40	0.33
Vancouver	52	94	31	0.33	0.41	0.36	0.20	0.20
Vienna	98	74	27	0.36	0.45	0.51	0.25	0.23
Warsaw	33	48	27	0.56	0.63	0.69	0.17	0.15
Washington	89	104	51	0.49	0.55	0.18	0.25	0.35

To better understand the relationships between different indicators, the Spearman correlation matrix for all variables is shown in Figure 5. Spearman correlation is chosen over Pearson due to non-linear relations between several pairs of variables. To examine in more detail the relations of the most significantly correlated pairs of variables with non-linear relationships, their scatter plots are shown in Figure 6.

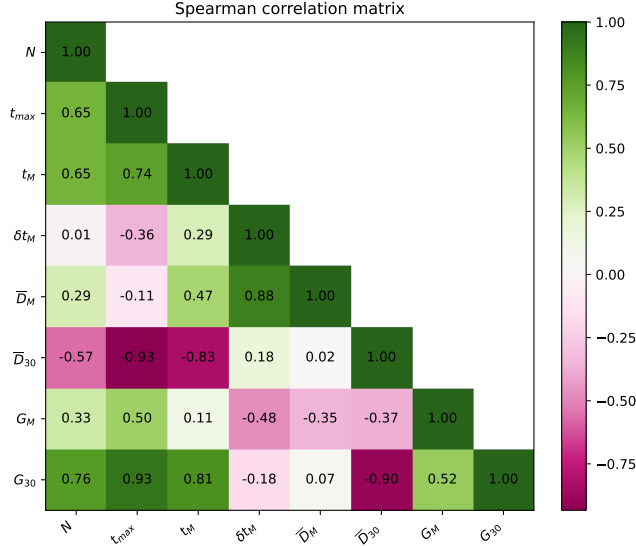


Figure 5: Spearman correlation matrix for accessibility variables. N : number of nodes in the network; t_{max} : maximum generalised travel time; t_M : time budget at maximal average degree growth; $\delta t_M = t_M/t_{max}$: t_M relative to maximum time; \bar{D}_M : average degree of the access graph at t_M ; \bar{D}_{30} : average degree of the access graph at $t_b = 30$ min; G_M : the Gini coefficient of the node degree distribution at t_M ; G_{30} : the Gini coefficient of the node degree distribution at $t_b = 30$ min.

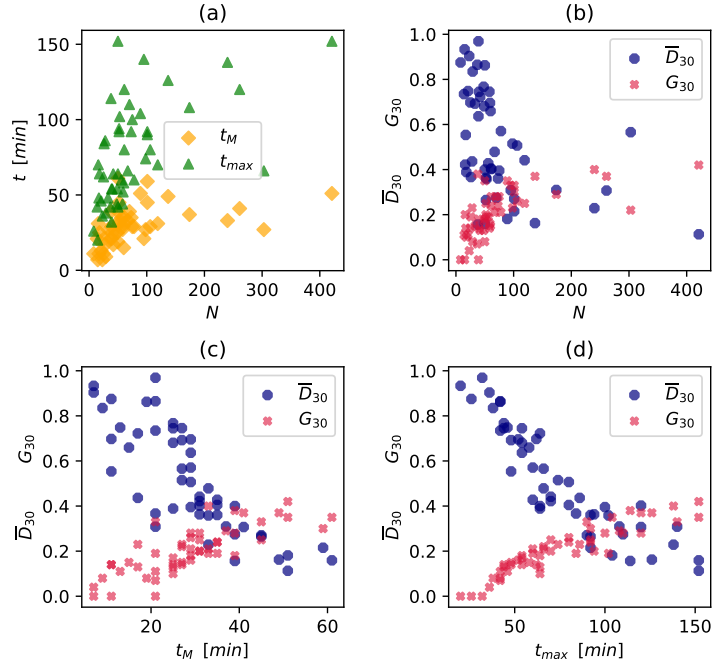


Figure 6: Scatter plots for selected pairs of variables with the highest observed values of Spearman correlation coefficients. In each subplot, one data point represents a separate network. (a) maximum travel time t_{max} and maximal growth time t_M vs. network size N . (b) average degree \bar{D}_{30} and Gini coefficient G_{30} at $t_b = 30$ min vs. N . (c) \bar{D}_{30} and G_{30} vs. t_M . (d) \bar{D}_{30} and G_{30} at $t_b = 30$ min vs. t_{max} .

The maximum travel time t_{max} varies for each city and increases approximately logarithmically with the size of the network N (Figure 6, plot (a)). Similarly to t_{max} , the time at maximum growth, t_M , increases sub-linearly with t_b , but converges much faster for large N , which is shown

in comparison in the same plot. This indicates a relatively better performance for larger networks. This is expected due to the approximately universal values of individual travel time budgets, and in PTN planning t_{max} must have a reasonable upper bound regardless of the size of the network. Note here that N is correlated with city geographical area and population size.

The values of the 30-min type indicators, the average degree \bar{D}_{30} and Gini coefficient G_{30} correlate significantly with the size of the network N , maximum growth time t_M and maximum generalised travel time t_{max} . The relations are shown in Figure 6 in plots (b), (c) and (d), respectively. Strong negative correlations and negative power-law relations are observed for \bar{D}_{30} . In contrast, the values of G_{30} increase logarithmically. For the largest networks, with size $N \gtrsim 150$, the value of the Gini coefficient is approximately constant, indicating that beyond a certain size, larger networks tend to offer equally unequal distributions of access, in contrast to the relation observed for small and moderately sized networks (i.e. the growth of G_M stalls after this N).

Among other pairs of variables, the strong negative correlation and a linear relation for \bar{D}_{30} and G_{30} complement the above observations. The high positive correlation and a linear relation between t_M and t_{max} is expected due to similar patterns of behaviour for all networks. Interestingly, the correlation of the absolute value of the time of fastest growth t_M and the value relative to maximum time $\delta t = t_M/t_{max}$ is relatively low ($r_S \approx 0.4$), suggesting the potential of using both values as accessibility indicators. Notable is the lack of correlation between δt_M and N , indicating a similar behaviour over all sizes of networks. On the other hand, the strong positive correlation between δt and the average degree at the time of fastest growth \bar{D}_M points to a universal behaviour of average degree growth (observed to be logistic-like in most cases). Moderate positive correlation of the Gini index of the degree distribution at t_M , G_M , and N , G_M and t_{max} indicate that larger networks also tend to have larger disparities in access. Significant negative correlation between the Gini index and δt indicates that inequity decreases with δt , complementing the previous observation on the relation to N .

4 Conclusions

We proposed a novel graph representation of public transport networks, the access graph \mathcal{G}_A . The edges in \mathcal{G}_A are based on shortest paths weighted with generalised travel times, as determined from the weighted L- and P-space representations, and directly connect nodes, reachable from one another within a given time budget. We studied the time budget-dependent topology of the access graph, specifically node degree evolution. Average degree and degree distributions of the access graphs for 51 metro networks were examined and a set of global accessibility indicators was proposed. First, the time budget at the fastest growth of average degree t_M , and average degree at this time, \bar{D}_M , along with the relative value of the maximal growth time to maximum travel time, δt_M , examine the access graph behaviour at a critical point. The Gini coefficient G_M of the degree distribution at the same value of time budget was used as an access equity indicator. These measures reflect network properties and can also be understood as network quality indicators. On the other hand, the value of the average degree \bar{D}_{30} and the Gini coefficient G_{30} at a fixed time budget of 30 minutes offer a complementary view from the passengers' perspective, offering a yardstick for comparing networks.

The introduced approach addresses an important gap in accessibility research. Our operationalisation of accessibility, based on graph theory and network science, contributes a methodology to unify accessibility studies. Instead of devising intricate metrics to include different properties of the transport system in the existing representations, we propose an algorithmic approach where each step is well-defined and the end result is a new graph representation where the simplest metric, the node degree, offers reliable, interpretable and transferable indicators. The widespread availability of the standardised GTFS timetable data format that can be used to build the standard PT graph representations, on which our methodology is based, makes the approach readily generalisable to analysis of other networks of all PT modalities. Importantly, the methodology can be applied with modifications of each step, for example, using different edge weights or different functions of distance, and arrive at similar definitions of indicators without compromising interpretability. Moreover, the similarity of behaviour of the proposed measures that was observed over all studied networks, supports the relevance of our approach for accessibility analysis.

We posit that the presented methodology offers a framework for unifying accessibility research, and opens important venues for in-depth exploration of accessibility. One of the limitations of the present study is the exclusion of land use data from the model, which will be instrumental in enhancing the analysis with information on the number of opportunities one can access from any given stop (e.g. number of households or workplaces). The following are proposed as some of the

most promising directions for future research: (i) incorporating land use and socio-demographic data into the model; (ii) detailed analyses of the t_b -varying connectedness and topology of the access graph; (iii) including information on access to and egress from the station; (iv) studying the impacts of disturbances on accessibility by means of simulations; (v) performing the same analysis for other transport modalities, such as bus, rail or tram networks, as well as road, bike and walk networks for comparative analyses of different modes of accessibility within a city, and; (vi) study the predictive power of the proposed indicators on ridership.

Table 3: Table of notations used.

Notation	Description
\mathcal{G}_A	access graph
N	number of nodes in the network
t_{max}	maximum generalised travel time
t_b	time budget
t_M	time budget at maximal growth of average degree
δt_M	t_M relative to t_{max} , t_M/t_{max}
\overline{D}	average degree of the access graph
\overline{D}_M	average degree of the access graph at $t_b = t_M$
\overline{D}_{30}	average degree of the access graph at $t_b = 30$ min
G	Gini coefficient
G_M	Gini coefficient of the degree distribution of the access graph at $t_b = t_M$
G_{30}	Gini coefficient of the degree distribution of the access graph at $t_b = 30$ min
w^{wait}	waiting time weight
$w^{transfer}$	transfer penalty
A	adjacency matrix
a_{ij}	element $[A]_{ij}$ of A
\mathcal{D}	generalised travel time matrix
d_{ij}	element $[\mathcal{D}]_{ij}$ of \mathcal{D}

Acknowledgements

The first and second author were partially supported by ARIS-Slovenian Agency for Research and Innovation (grants P2-0394 (A) and P1-0222, respectively, and grant SN-ZRD/22-27/0510 for both authors).

References

- Adjetey-Bahun, K., Birregah, B., Châtelet, E., & Planchet, J.-L. (2016). A model to quantify the resilience of mass railway transportation systems. *Reliability Engineering & System Safety*, 153, 1–14.
- Ahmed, A., & Stopher, P. (2014). Seventy minutes plus or minus 10—a review of travel time budget studies. *Transport Reviews*, 34(5), 607–625.
- Bittencourt, T. A., & Giannotti, M. (2023). Evaluating the accessibility and availability of public services to reduce inequalities in everyday mobility. *Transportation research part A: policy and practice*, 177, 103833.
- Cats, O. (2016). The robustness value of public transport development plans. *Journal of Transport Geography*, 51, 236–246.
- Cats, O. (2017). Topological evolution of a metropolitan rail transport network: The case of stockholm. *Journal of Transport Geography*, 62, 172–183.
- Cats, O., Koppenol, G.-J., & Warnier, M. (2017). Robustness assessment of link capacity reduction for complex networks: Application for public transport systems. *Reliability Engineering & System Safety*, 167, 544–553.
- Cats, O., & Krishnakumari, P. (2020). Metropolitan rail network robustness. *Physica A: statistical mechanics and its applications*, 549, 124317.

- Cui, M., & Levinson, D. (2020). Primal and dual access. *Geographical Analysis*, 52(3), 452–474.
- de Regt, R., von Ferber, C., Holovatch, Y., & Lebovka, M. (2019). Public transportation in great britain viewed as a complex network. *Transportmetrica A: Transport Science*, 15(2), 722–748.
- Derrible, S., & Kennedy, C. (2011). Applications of graph theory and network science to transit network design. *Transport reviews*, 31(4), 495–519.
- Dimitrov, S. D., & Ceder, A. A. (2016). A method of examining the structure and topological properties of public-transport networks. *Physica A: Statistical Mechanics and its Applications*, 451, 373–387.
- Ding, R., Ujang, N., Hamid, H. B., Manan, M. S. A., Li, R., Albadareen, S. S. M., ... Wu, J. (2019). Application of complex networks theory in urban traffic network researches. *Networks and Spatial Economics*, 19, 1281–1317.
- Dupuy, G. (2013). Network geometry and the urban railway system: the potential benefits to geographers of harnessing inputs from “naive” outsiders. *Journal of Transport Geography*, 33, 85–94.
- El-Geneidy, A., Levinson, D., Diab, E., Boisjoly, G., Verbich, D., & Loong, C. (2016). The cost of equity: Assessing transit accessibility and social disparity using total travel cost. *Transportation Research Part A: Policy and Practice*, 91, 302–316.
- Geurs, K. T., & Van Wee, B. (2004). Accessibility evaluation of land-use and transport strategies: review and research directions. *Journal of Transport geography*, 12(2), 127–140.
- GoogleDevelopers. (2025). *General transit feed specification (gtfs)*. Retrieved from <https://developers.google.com/transit/gtfs> (Accessed: 2025-02-01)
- Gori, S., Mannini, L., & Petrelli, M. (2020). Equity measures for the identification of public transport needs. *Case Studies on Transport Policy*, 8(3), 745–757.
- Hagberg, A., Swart, P. J., & Schult, D. A. (2008). *Exploring network structure, dynamics, and function using networkx* (Tech. Rep.). Los Alamos National Laboratory (LANL), Los Alamos, NM (United States).
- Hansen, W. G. (1959). How accessibility shapes land use. *Journal of the American Institute of planners*, 25(2), 73–76.
- Karner, A. (2018). Assessing public transit service equity using route-level accessibility measures and public data. *Journal of Transport Geography*, 67, 24–32.
- Lahoorpoor, B., Rayaprolu, H., Wu, H., & Levinson, D. M. (2022). Access-oriented design? disentangling the effect of land use and transport network on accessibility. *Transportation Research Interdisciplinary Perspectives*, 13, 100536.
- Levinson, D., & Wu, H. (2020). Towards a general theory of access. *Journal of Transport and Land Use*, 13(1), 129–158.
- Luo, D., Cats, O., & van Lint, H. (2020). Can passenger flow distribution be estimated solely based on network properties in public transport systems? *Transportation*, 47(6), 2757–2776.
- Luo, D., Cats, O., van Lint, H., & Currie, G. (2019). Integrating network science and public transport accessibility analysis for comparative assessment. *Journal of Transport Geography*, 80, 102505.
- Musso, A., Vuchic, V. R., et al. (1988). *Characteristics of metro networks and methodology for their evaluation*. National Research Council, Transportation Research Board Washington, DC, USA.
- Neutens, T. (2015). Accessibility, equity and health care: review and research directions for transport geographers. *Journal of Transport Geography*, 43, 14–27.
- Šfiligoj, T., Peperko, A., Bajec, P., & Cats, O. (2025). Node importance corresponds to passenger demand in public transport networks. *Physica A: Statistical Mechanics and its Applications*, 130354.

- Vijlbrief, S., Cats, O., Krishnakumari, P., van Cranenburgh, S., & Massobrio, R. (2022a). *A curated data set of l-space representations for 51 metro networks worldwide*. 4TU.ResearchData. Retrieved from https://data.4tu.nl/articles/dataset/A_curated_data_set_of_L-space_representations_for_51_metro_networks_worldwide/21316824/1 doi: 10.4121/21316824.v1
- Vijlbrief, S., Cats, O., Krishnakumari, P., van Cranenburgh, S., & Massobrio, R. (2022b). *A curated data set of p-space representations for 51 metro networks worldwide*. 4TU.ResearchData. Retrieved from https://data.4tu.nl/articles/dataset/A_curated_data_set_of_P-space_representations_for_51_metro_networks_worldwide/21316950/2 doi: 10.4121/21316950.v2
- Von Ferber, C., Holovatch, T., Holovatch, Y., & Palchykov, V. (2009). Public transport networks: empirical analysis and modeling. *The European Physical Journal B*, 68, 261–275.
- Vuchic, V. R., & Musso, A. (1991). Theory and practice of metro network design. *Public transport international*, 40(3), 298.
- Wu, H., Avner, P., Boisjoly, G., Braga, C. K., El-Geneidy, A., Huang, J., ... others (2021). Urban access across the globe: an international comparison of different transport modes. *npj Urban Sustainability*, 1(1), 16.
- Yap, M., Wong, H., & Cats, O. (2024). Passenger valuation of interchanges in urban public transport. *Journal of Public Transportation*, 26, 100089.